Journal of Virological Methods 236 (2016) 93–97

Contents lists available at ScienceDirect

Journal of Virological Methods

journal homepage: www.elsevier.com/locate/jviromet

Short communication

Detection of Zika virus by SYBR green one-step real-time RT-PCR

Ming-Yue Xu[a,b,1], Si-Qing Liu[a,1], Cheng-Lin Deng[a], Qiu-Yan Zhang[a,b], Bo Zhang[a,*]

[a] Key Laboratory of Special Pathogens and Biosafety, Center for Emerging Infectious Diseases, Wuhan Institute of Virology, Chinese Academy of Sciences, Wuhan 430071, China
[b] University of Chinese Academy of Sciences, Beijing 100049, China

Article history:
Received 11 May 2016
Received in revised form 8 July 2016
Accepted 15 July 2016
Available online 18 July 2016

Keywords:
Zika virus
Real-time RT-PCR
SYBR green

A B S T R A C T

The ongoing Zika virus (ZIKV) outbreak has rapidly spread to new areas of Americas, which were the first transmissions outside its traditional endemic areas in Africa and Asia. Due to the link with newborn defects and neurological disorder, numerous infected cases throughout the world and various mosquito vectors, the virus has been considered to be an international public health emergency. In the present study, we developed a SYBR Green based one-step real-time RT-PCR assay for rapid detection of ZIKV. Our results revealed that the real-time assay is highly specific and sensitive in detection of ZIKV in cell samples. Importantly, the replication of ZIKV at different time points in infected cells could be rapidly monitored by the real-time RT-PCR assay. Specifically, the real-time RT-PCR showed acceptable performance in measurement of infectious ZIKV RNA. This assay could detect ZIKV at a titer as low as 1 PFU/mL. The real-time RT-PCR assay could be a useful tool for further virology surveillance and diagnosis of ZIKV.

In May 2015, local transmitted infection following the identification of Zika virus (ZIKV) in eight patients was firstly reported in Brazil (Kindhauser et al., 2016; Zanluca et al., 2015). Since then, the virus rapidly spread to more than 20 countries and territories (Kindhauser et al., 2016), and approximately 1.5 million cases of ZIKV infections were estimated in Brazil alone (Lazear and Diamond, 2016). Although most of ZIKV-infected cases are asymptomatic or only developed mild clinical symptoms characterized by fever, skin rash, joint pain, or conjunctivitis, increasing evidence suggests that the ZIKV infection is associated with neurologic disorders and congenital malformations (i.e. Guillain–Barré syndrome and microcephaly) (Besnard et al., 2014; Calvet et al., 2016; Chang et al., 2016; Mlakar et al., 2016; Oehler et al., 2014).

ZIKV is a member of *Flavivirus* genus which includes many other important pathogens such as dengue virus (DENV), West Nile virus (WNV), yellow fever virus (YFV), and Japanese encephalitis virus (JEV) (Kuno et al., 1998). It is transmitted to people mainly through the bite of an infected *Aedes* spp. mosquito, for example *Ae. africanus*, *Ae. aegypti*, and *Ae. furcifer* (Diallo et al., 2014; Dick et al., 1952; Marchette et al., 1969), the same vectors that transmit other arboviruses such as YFV, DENV, and chikungunya virus (CHIKV) (Gubler, 1998). Besides, the clinical symptoms of Zika fever resembles other tropic infectious diseases, especially those caused by DENV and CHIKV, which could increase the rate of misdiagnoses for ZIKV infections. Some studies have indicated that ZIKV is following the migration pattern of DENV and CHIKV, spreading to regions and countries infested with the common mosquito vectors (Musso et al., 2015; Shen et al., 2016). Additionally, the increasing imported cases of ZIKV infection to countries where ZIKV is not endemic could further make the biogeography pattern and epidemic dynamics complicated and uncontrollable. Therefore, the current situation highlights the importance of surveillance for ZIKV, the urgency for exploring replication mechanism, and the need for specific detection of this virus.

In this paper, we developed a highly sensitive and specific approach for detection of ZIKV by using SYBR Green based one step real-time RT-PCR analysis. The ZIKV-specific primers were designed based on the conserved regions placed between the NS5 and 3′UTR genes of ZIKV. The primer pairs are ZIKV-F: 5′-AGGATCATAGGTGATGAAGAAAAGT-3′ and ZIKV −R: 5′-CCTGACAACACTAAGATTGGTGC-3′ (Fig. 1). Sequences from the closely related mosquito-borne viruses Spondweni virus (SPOV), DENV1-4, JEV, WNV, and YFV were used to avoid cross-reactivity of the ZIKV primers as well. (Fig. 1). Real time RT-PCR assay in this study was performed using one step SYBR green PrimeScript PLUS RT-PCR kit (TaKaRa) with the following amplification conditions:

* Corresponding author.
E-mail address: zhangbo@wh.iov.cn (B. Zhang).
[1] Both the authors contributed equally to this work.

http://dx.doi.org/10.1016/j.jviromet.2016.07.014
0166-0934/

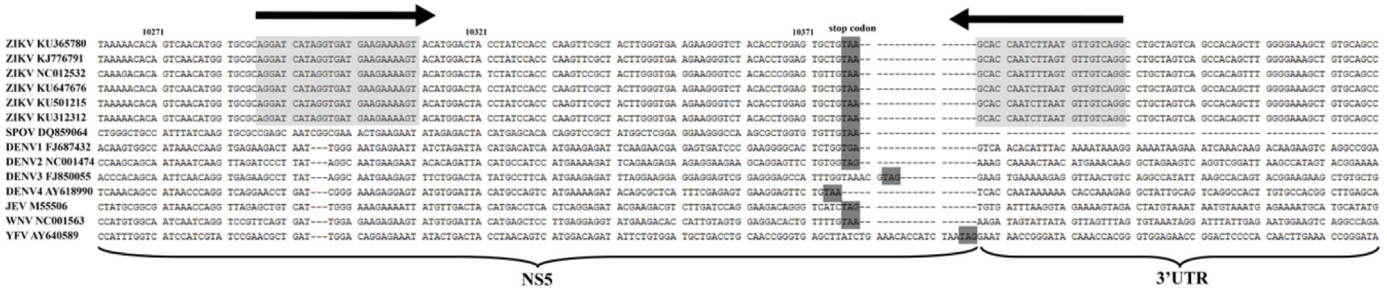

Fig. 1. Sequences alignment of ZIKV related mosquito-borne flaviviruses for partial NS5 and 3′UTR genes. Primer sequences are highlighted in light gray fields. Gaps are presented as hyphens. Stop codon of NS5 genes were indicated by dark gray boxes. The arrows show the orientation of primers in 5′ to 3′ direction. Only six representative strains of ZIKV were selected in the map of primer sequences alignment.

42 °C for 5 min, 95 °C for 10 s and 40 cycles of 95 °C for 5 s, 60 °C for 34 s.

First of all, a standard curve was generated by using the 10-fold serial dilutions of in vitro transcribed viral genomic RNA ranging from 15 to 1.5×10^8 copies/μL. The regression line was established by plotting the threshold cycles (C_T) values against the copy number of RNA transcripts. As shown in Fig. 2A, the standard curve covered a linear range of six orders of magnitude, for which the slopes were −3.742, and $R^2 = 0.997$. It was demonstrated that the SYBR Green real-time RT-PCR assay was feasible for the quantification of ZIKV in samples.

Specificity was evaluated by testing in vitro transcribed RNAs from flaviviruses DENV2, JEV, WNV, and Omsk hemorrhagic fever virus (OHFV) isolates, as well as an alphavirus CHIKV isolate. The full-length cDNA clones of JEV (Li et al., 2014), DENV2, WNV, and CHIKV (unpublished data) were constructed in our laboratory, and that of OHFV (Yoshii et al., 2011) was generous gift. For assessment of specific amplification, RNA templates were tested at the same quantity of precisely 1.0 ng per reaction. Equal amounts of transcribed RNAs of ZIKV and all other related viruses were evaluated by our developed ZIKV real-time RT-PCR assay. The ZIKV-F and ZIKV-R primers were highly specific. As it is shown in Fig. 2B, the C_T values of all those viruses were more than 34 while the C_T value of ZIKV was approximately 15.92. Moreover, only a background signal was detected in the negative control without a RNA template.

To evaluate the sensitivity of the ZIKV real-time RT-PCR assay, a dilution range from 10.0 to 10^{-2} ng/μL of the ZIKV RNA combined with the 200 ng of Vero cells RNA were tested by the primer pairs. The result demonstrated that the sensitivity of this assay was only slightly affected in the presence of such high amount of cellular RNA (*T-test*, $P > 0.05$) (Fig. 2C). This result indicated that the addition of cellular RNA did not alter the detection efficiency of ZIKV RNA.

Recently, the newly developed real-time RT-PCR has been used for the detection of the isolate of ZIKV SZ-WIV01 strain (KU963796) derived from an imported human case in China (Deng et al., 2016). The original serum sample from the infected patient was blindly passaged three times on C6/36 cells (P1–P3). The results indicated that genomic RNA copies of ZIKV were significantly increased in C6/36 cells with the serial passage (Fig. 3). For convenience, the obtained infectious ZIKV derived from P3 passage is designated as WT ZIKV and used in the following experiments.

We firstly analyzed the growth dynamics of WT ZIKV in Vero cells. Vero cell monolayers cultured in 35 mm culture dishes were infected with WT ZIKV (MOI of 0.1) at 70–80% confluence. The viral supernatants were harvested at different times post-infection (Fig. 4A). The viral titers were quantified by plaque assay. The viral RNAs (vRNA) were extracted from 140 μL viral supernatants using QIAamp Viral RNA Mini Kit (Qiagen) following the manufacturer's instructions. The vRNA extracts were then resuspended in 60 μL of buffer AVE, of which 6.4 μL were used as template in the 20 μL reaction system of real-time RT-PCR. Growth curves obtained from plaque assay and real-time RT-PCR methods were compared. The virus titers of infectious ZIKV were well correlated with the copy numbers of ZIKV genomic RNA, and a strong linear correlation was observed between them ($R^2 = 0.957$; $P < 0.05$) (Fig. 4B). The mean peak viral titer of 1.4×10^6 PFU/mL was observed at 120 h post-infection for plaque assay. Accordingly, the maximum copy number of genomic RNA (3.9×10^8 copies/μL) was also obtained at the same time point by real-time RT-PCR (Fig. 4A). It should be noted that the RNA copy number in the supernatants was larger than the titer of the virus determined by plaque assay. This phenomenon was also observed for other viruses in previous studies in which the ratios of RNA copy number to viral titer ranging from 2 to 3 log units or more (Bae et al., 2003; Garcia et al., 2001; Guillaume et al., 2004; Houng et al., 2000; Richardson et al., 2006). The discrepancy could be attributed to the accumulation of defective particles and free viral RNA released from ruptured infected cells during viral infection (Guillaume et al., 2004). Altogether, the real-time RT-PCR assay can be used to characterize the replication of ZIKV at different time points post-infection in cells.

In order to further investigate the performance of the real-time RT-PCR in quantification of viral load in samples, linear curve was generated from ZIKV RNA extracted from 10-fold diluted virus stock with known viral titers (highest virus titer at 120 hpi, Fig. 4A) in triplicate. The developed real-time RT-PCR assay showed a linear curve with high amplification efficiency and strong correlation ($R^2 = 0.996$, Fig. 4C). Here, we could establish a linear relation between the log number of viral genome molecules (infectious viral particles plus all other non-infectious viral molecules) (Fig. 2A) and that of infectious virus (infectious viral particles only) (Fig. 4C) by using the common dependent variable (i.e. CT values). Based on our calculation, each infectious plaque forming unit (PFU) is roughly equal to 2×10^5 RNA genome copies. The ratio of RNA copies to PFU for ZIKV was obviously high. Compared with other flaviviruses (Fayzulin et al., 2006; Li et al., 2016; Shin et al., 2013), the highest viral titer that ZIKV can reach up to was relatively lower (Fig. 4A) in mammalian cells, which could lead to the generation of high amount of non-infectious particles or free viral RNA genomes in cultural supernatants. In this regards, these non-infectious molecules might in turn increase the ratio of RNA copies to PFU. Thus, further studies will be necessary to identify what has an implication on the differences of multiplication between ZIKV and other flaviviruses in mammalian cells.

Besides, we established the detection limit of this assay system using the minimum level of 100 PFU/mL in linearity study as a starting concentration. The serial diluted concentrations of ZIKV (100, 50, 10, 5, 1, 0.1 PFU/mL) were tested in a single run in triplicate in three independent experiments. The amplification curves of the ZIKV RNA extracts from six dilutions are shown in Fig. 4D. The real-time RT-PCR detected as low as 1 PFU/mL in ZIKV RNA extracts (C_T